EFDA
EUROPEAN FUSION DEVELOPMENT AGREEMENT
JET

EFDA–JET–CP(03)01-01

P. Andrew, W. Fundamenski, A. Huber, P.J. Lomas, G. Matthews, J. Paley,
V. Riccardo and JET EFDA Contributors

Heat Load to the JET Divertor During Disruptions and Disruption Mitigation by Massive Gas Puffing

Heat Load to the JET Divertor During Disruptions and Disruption Mitigation by Massive Gas Puffing

P. Andrew[1], W. Fundamenski[1], A. Huber[1], P. J. Lomas[1], G. Matthews[1], J. Paley[2], V. Riccardo[1] and JET EFDA Contributors

[1]EURATOM/UKAEA Fusion Association, Culham Science Centre, Abingdon, UK
[2]Imperial College London, Prince Consort Road, London, UK
**See Annex of J. Pamela et al., "Overview of Recent JET Results and Future Perspectives", Fusion Energy 2000 (Proc. 18th Int. Conf. Sorrento, 2000), IAEA, Vienna (2001).*

Preprint of Paper to be submitted for publication in Proceedings of the
EPS Conference on Controlled Fusion and Plasma Physics,
(St. Petersburg, Russia, 7-11 July 2003)

INTRODUCTION

Dedicated JET experiments have focused on heat flow to the divertor during disruptions and disruption mitigation by impurity puffing. Planned disruptions backed up the earlier observation [1] that most of the stored thermal energy is not deposited in the divertor during the thermal quench. Attempts to disrupt plasmas with large gas puffs simply resulted in density limit disruptions, probably because our gas injection system was not fast enough.

1. DIVERTOR HEAT LOAD DURING DISRUPTIONS

The thermal quench phase of a disruption results in a high power heat pulse where essentially all the plasma thermal energy, $E_{thermal}$, can be transferred to walls in <1msec [2]. If during the thermal quench $E_{thermal}$ is deposited in the steady state strike zones, the heat load will be many times larger than for a type-I ELM, because the whole plasma stored energy is involved, not just a few percent. The ITER design assumes such a power load resulting from a thermal quench, but spread over a 3× larger power footprint [3].

Experimental results on energy deposited during the thermal quench varies widely from experiment to experiment. In TEXTOR, more than 50% of Ethermal is seen in a power footprint similar to steady state [4]. Both ASDEX & DIII-D report more than 50% of $E_{thermal}$ in divertor, but broader than steady-state strike power footprints [5]. In contrast, JET observes < 50%, and often <20% of $E_{thermal}$ in the divertor.

The JET result hinges on IR measurements over ~6% of the divertor toroidal circumference. In contrast, the JET IR system sees all the energy going to the divertor during steady state and >50% during ELM's. Thermocouple measurements [1] support the apparent energy deficit during disruptions, and suggests toroidal asymmetry is peculiar to runaway electron events. Finally, if toroidal asymmetry was an issue, the IR should have seen cases with >100% energy to the divertor.

To address the lack of energy arriving in the JET divertor, dedicated experiments were performed on JET optimised for divertor heat pulse observations. First, a configuration with relatively high wall clearance was adopted; the minimum separatrix/wall distance was increased to 12cm (normally 4cm is typical). This was done to decrease the chance of power being scraped off in the main chamber due to possible changes in the equilibrium during the thermal quench. Generally, magnetic reconstructions of the plasma position indicate that plasma remains in a divertor configuration during the thermal quench. Usually JET operates with a protection system to decrease the plasma shaping when an n = 2 mode is detected. This was disabled during the planned disruptions for similar concerns of losing divertor configuration. Finally, the divertor strike points were positioned to give the best view of the strike zones for infra-red measurement of the target temperature.

Figure 1 illustrates a planned disruption triggered by lowering the toroidal field to the point where q = 2 is at the plasma surface. The plasma thermal energy as measured by a diamagnetic loop, $E_{thermal}$, is unreliable immediately following the thermal quench (dashed line), so a core ECE electron temperature measurement is shown as well. The integrated power to the divertor during the disruption, as measured by IR thermography, increased due to the steady state power out of the plasma, and takes an ~0.3MJ step during the disruption. This should be compared to the prompt 0.85MJ stored energy loss at the thermal quench.

The pulse in Fig.2 was run at higher density, so that a β limit was reached. However, this disruption is preceeded by a locked mode appearing 0.25sec before the thermal quench. Typically, just prior to the thermal quench, there can be a drop in plasma thermal energy due to relatively slow events (e.g. H-L transitions, appearance of a locked mode). Most of thermal energy associated with these slow losses appears in the divertor.

The JET bolometer system is generally not fast enough to time-resolve thermal quench and current quench. A single channel fast (τ = 0.5msec) bolometer shows most of radiation appearing too late to be due to the thermal quench (Fig.3), suggesting that radiation is not a significant loss channel during the thermal quench.

The implication is that energy is lost to the main chamber wall during the thermal quench. An analogous situation exists with ELM's, but involving a smaller fraction of the energy lost from the plasma [6,7]. Unfortunately, JET is not currently equipped to directly measure heat flux to the main chamber. There is, however, circumstantial evidence of interaction with the main chamber during the thermal quench. Firstly, during the thermal quench, both limiter and divertor Langmuir probes see large current spikes (Fig.3). The two Langmuir probe currents have different sign merely because the oscillating bias voltages are out of phase at the time of the thermal quench.

Another indication of interaction with the wall , in some disruption classes (eg ITB plasmas), is the electron temperature profile prior to the disruption (Fig.4). Because the plasma is rotating, the radial excursion of the hot plasma in time is interpreted as a distortion in the flux surfaces rotating past the measurement point. The rotation is supported by magnetic measurements. This distortion extends more than 10cm radially in the 500μsec interval leading up to the thermal quench [8].

2. DISRUPTION MITIGATION BY MASSIVE GAS PUFFING

Disruptions result in high thermal and mechanical loads on the vacuum vessel [5]. Massive gas puffing has been used successfully on other experiments to mitigate halo current forces, runaway electrons and the heat pulse from the thermal quench [9].

JET has performed a disruption mitigation experiment using He, Ne and Ar puffs. The existing gas introduction valve delivers up to 2×10^{22} atoms in 50μsec puff. Planned disruptions were achieved by disabling the vertical stabilisation resulting in a vertical displacement event (VDE). No disruption detection network was used. The relative timing of the gas puff and VDE was achieved by trial and error. Figure 5 illustrates the result that He puffs slowed down the current quench, while Ne and Ar accelerated the current quench relative to a disruption with no puff (pure VDE). This is consistent with higher z resulting in a lower Te, hence larger plasma resistivity and shorter L/R time. A prompt current decay results in smaller plasma current vertical moment Ip•Δz (Fig.5), i.e. the current decays before a larger vertical displacement can occur. ∫Ip•Δzdt is a measure of the impulse to the vessel due to halo current forces balancing the vertical stabilising force, and indeed scales with the vertical force on the vessel supports (Fig.6).

However, it was found that the same result could be achieved using a much smaller gas puff; i.e. just enough to cause a density limit. We conclude that the gas puff system used is too slow to mimic the DIII-D results, but that triggering a density limit disruption substantially reduces the forces on the vessel.

CONCLUSIONS

In JET, typically more than 50% (often >80%) of plasma thermal energy does not appear in the divertor during a disruption. Radiation is not the loss channel for the missing energy. Instead, interaction with the main chamber walls is suspected, despite evidence that the plasma remains in a divertor configuration.

Neon and Argon gas puffs used on JET were successful in reducing halo current forces. Dedicated experiments confirmed, however, that a faster gas delivery system will be required to mitigate the thermal quench.

ACKNOWLEDGEMENTS

This work was conducted under the European Fusion Development Agreement and funded in part by the UK Engineering & Physical Sciences Research Council and EURATOM

REFERENCES

[1]. V. Riccardo et al, Plasma Phys. Contr. Fus. **44** (2002) 905-929.
[2]. J.A. Wesson et al, Nucl. Fus. **29** (1989) 641
[3]. G. Federici et al, J. Nucl. Mater. 313-316 (2003) 11
[4]. Ciotti et al, J. Nucl. Mater. 266-269 (1999) 1023
[5]. V. Riccardo, these proceedings
[6]. A. Hermann et al, J. Nucl. Mater. 313-316 (2003) 759
[7]. W. Fundamenski, submitted to Plasma Phys. Contr. Fus.
[8]. S. Cowley, these proceedings
[9]. D. Whyte et al, J. Nucl. Mater. 313-316 (2003) 1239

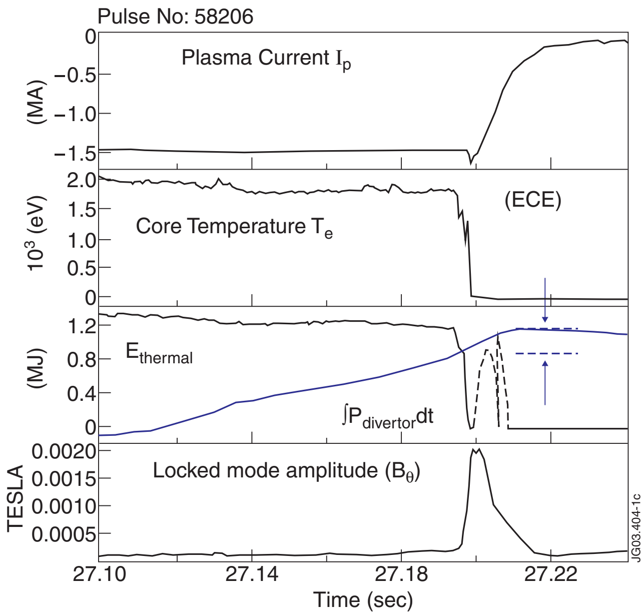

Figure 1. A q = 2 disruption: the integrated power to the divertor during the thermal quench ~0.3MJ, i.e 35% $E_{thermal}$ (Pulse No: 58206).

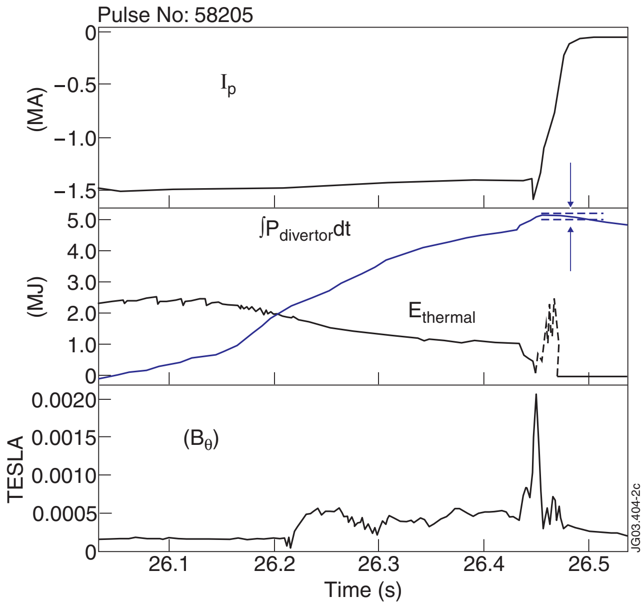

Figure 2. A β-limit disruption: thermal energy lost during ELM's [2] and locked mode preceeding disruption go to divertor, but only 50% at thermal quench. (Pulse No: 58205).

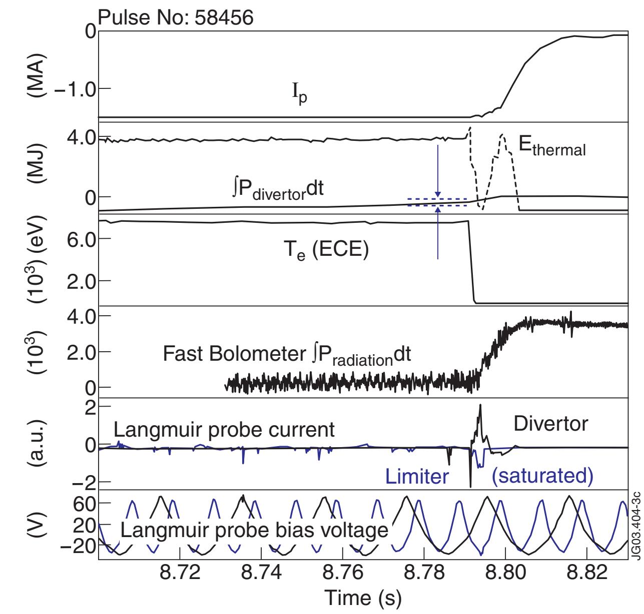

Figure 3. Disruption of an ITB discharge. Energy loss by radiation mainly after thermal quench. During thermal quench, energy to divertor is 15% $E_{thermal}$. (Pulse No: 58456).

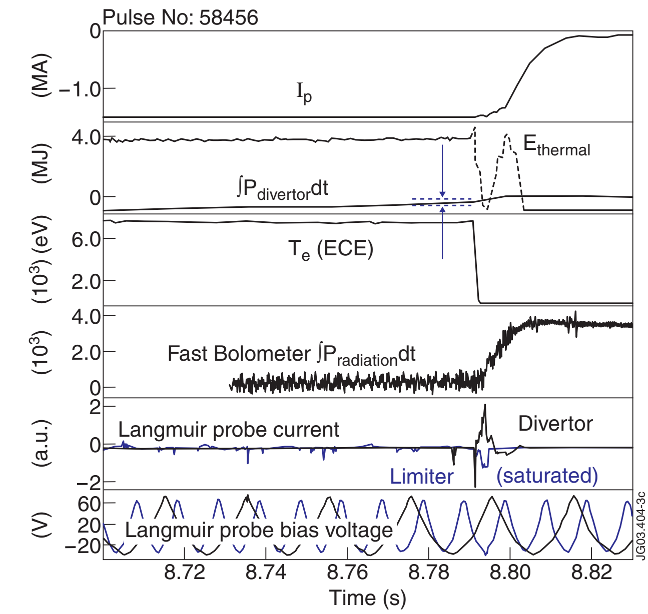

Figure 4. Electron temperature contour plot for an ITB plasma at the thermal quench, measured by ECE. Ovals indicate successive rotations of the extended hot plasma past the measurement point. (Pulse No: 58673).

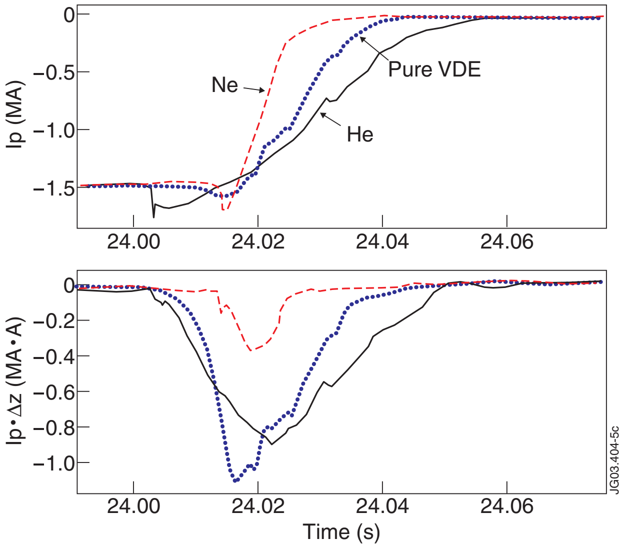

Figure 5. 3 disruptions of a similar plasma configuration. Disruptions caused by a) He puff, b) Ne puff, and c) disabling vertical stabilisation. Plasma current (above) and plasma current vertical moment (below).

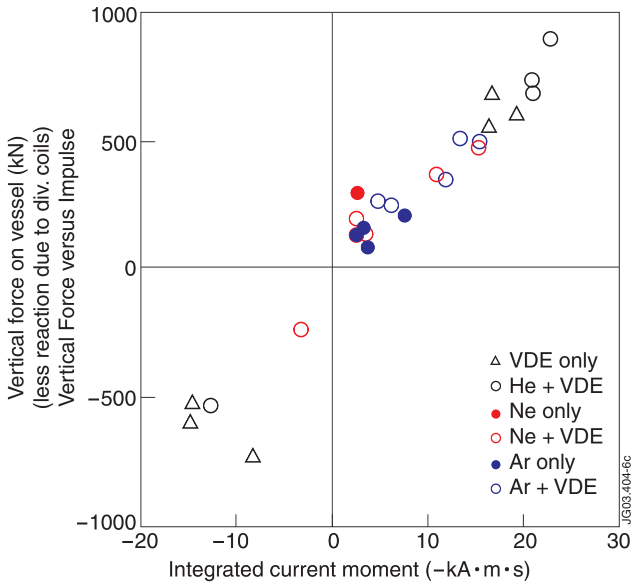

Figure 6. Vertical force on vacuum vessel during disruptions (similar plasma current and configuration) vs ∫Ip• Δzdt. The force due to the divertor coils themselves, which are supported by the vessel, has been subtracted from the vessel force.